



Brazilian Journal of Physics

ISSN: 0103-9733

luizno.bjp@gmail.com

Sociedade Brasileira de Física
Brasil

Mohammadyani, Dariush; Modarress, Hamid; C. To, Alber; Amani, Amir
Interactions of Fullerene (C60) and its Hydroxyl Derivatives with Lipid Bilayer: A Coarse-Grained
Molecular Dynamics Simulation
Brazilian Journal of Physics, vol. 44, núm. 1, 2014, pp. 1-7
Sociedade Brasileira de Física
São Paulo, Brasil

Available in: <http://www.redalyc.org/articulo.oa?id=46429745001>

- How to cite
- Complete issue
- More information about this article
- Journal's homepage in redalyc.org

redalyc.org

Scientific Information System
Network of Scientific Journals from Latin America, the Caribbean, Spain and Portugal
Non-profit academic project, developed under the open access initiative

Interactions of Fullerene (C₆₀) and its Hydroxyl Derivatives with Lipid Bilayer: A Coarse-Grained Molecular Dynamics Simulation

Dariush Mohammadyani · Hamid Modarress ·
Alber C. To · Amir Amani

Received: 14 May 2013 / Published online: 11 December 2013
© Sociedade Brasileira de Física 2013

Abstract Coarse-grained molecular dynamic simulations were employed to study the interactions of fullerene (C₆₀) and its hydroxyl derivatives (C₆₀(OH)_n, $n=4, 5, 6, 8, 12$, and 16) with a lipid bilayer composed of dipalmitoylphosphatidylcholine molecules. It was found that the C₆₀ moves towards the center of the bilayer and laid between central and peripheral regions of the bilayer. The potential mean force was calculated to estimate free energy profile when pulling the fullerene from its initial position to the center of the bilayer using an umbrella sampling method. Results showed that the hydrophobic region of the membrane acts as a barrier to transport a nonpolar C₆₀ molecule through the bilayer. This makes a deep minimum in the free energy profile between the center and head regions of membrane. Various numbers of polar functional groups (–OH) were then used to make derivatives of fullerene and change the hydrophilic of the molecule. It was found that optimal number of hydroxyl groups to facilitate the transportation of C₆₀(OH)_n through the bilayer is 4.

D. Mohammadyani (✉)
Department of Bioengineering, University of Pittsburgh,
Pittsburgh, PA, USA
e-mail: d.mohammadyani@gmail.com

H. Modarress
Department of Chemical Engineering,
Amirkabir University of Technology, Tehran, Iran

A. C. To
Department of Mechanical Engineering and Material Science,
University of Pittsburgh, Pittsburgh, PA, USA

A. Amani (✉)
Department of Medical Nanotechnology,
School of Advanced Technologies in Medicine,
Tehran University of Medical Sciences, Tehran, Iran
e-mail: aamani@sina.tums.ac.ir

A. Amani
Medical Biomaterials Research Center,
Tehran University of Medical Sciences, Tehran, Iran

Keywords Fullerene (C₆₀) · Lipid bilayer · Molecular dynamic simulation

1 Introduction

Fullerene has shown promising capabilities in biomedical applications such as photodynamic therapy and antioxidant/antiviral activities [1–3]. For instance, its potential of enzyme inhibition and DNA cleavage has been reported [4]. Such capabilities along with applications in drug and gene delivery systems have attracted the attention of a large number of biomedical researchers [5–7].

Nevertheless, the solubility of fullerene in aqueous solvents and biological media is known to be quite low, hampering its utilization in biology [4, 8]. Experimental studies have shown that chemical functionalization of fullerene is able to increase the solubility of fullerene in biological environments. Therefore, functionalization of fullerene may allow design of new materials with superior performance. Additionally, the toxicity of fullerenes that has been documented to be related to their solubility in water—the cytotoxicity of functionalized fullerenes with high water solubility is normally less than that of C₆₀ [9].

Another concern to employ fullerene in medicine is its lack of ability to pass through cell membranes to enter a living cell. Therefore, another advantage of functionalization is to help fullerene pass through a cell membrane. Chang et al. [10] have experimentally studied the interaction of C₆₀(C(COOH)₂)₂ with living cells and showed that this particle was able to enter the cell. They also showed that crossing the cell membrane is a time and energy consuming process. Furthermore, it was mentioned that the carboxylated fullerene is able to deliver fluorescein, a molecule that cannot normally cross cell membranes.

In recent years, computational studies have been carried out to understand the mechanism of cells taking up fullerenes and its derivatives. Several approaches have been used in this area,

e.g., Li et al. [11] and Qiao et al. [12] used all-atoms molecular simulations (AA-MD) to determine the equilibrium position of a single C_{60} molecule in a dimyristoylphosphatidylcholine (DMPC) and a dipalmitoylphosphatidylcholine (DPPC) lipid bilayers, respectively. The position was $\sim 6\text{--}7$ Å off the bilayer center. Their results were in agreement with that of Bedrov et al. [13], which showed that the minimum free energy is observed at $\sim 6\text{--}7$ Å off-center of the DPPC bilayer. The interactions of C_{60} and functionalized C_{60} with 20 hydroxyl groups with a DPPC bilayer have also been investigated using interatomic potentials [12]. In the latter work, the potential mean force (PMF) profiles of the fullerene and its derivative for translocation across the bilayer have been compared.

Since the accessible temporal and spatial scales limit AA-MD simulations, coarse-grained (CG) MD has been introduced as an alternative to increase computational efficiency, especially for simulating super biomolecules. CG-MD can actually reach the scale of current experimental techniques [14, 15]. In this case, D'Rozario et al. [16] used CG-MD to study the interactions of C_{60} and its derivatives with DPPC lipid bilayer. They used 3 to 1 mapping and considered 20 beads for fullerene and found that the number of functional groups had a significant effect on the nature of the interactions with the lipid bilayer. They showed that fullerene penetrates inside DPPC and is located in the center of lipid bilayer with a deep valley in free energy profile in the center of the DPPC. In another study, Wong-Ekkabut et al. [17] used the MARTINI force field to study the interactions of C_{60} with dioleoylphosphatidylcholine and DPPC lipid. Their work comprised employing 4 to 1 mapping and proposing a new force field for fullerene. They reported the effect of agglomeration on the mechanical properties of the bilayer. Although a considerable number of reports are available on the interaction of fullerenes with cell membrane, only one study has tried working on the optimization of fullerene derivatives [12]. No report so far has identified the structure of a fullerene hydroxyl derivative optimized to cross the lipid bilayer.

The aim of this study is to investigate the interactions of fullerene and its hydroxyl derivatives with the DPPC lipid bilayer and to find optimal number of the hydroxyl functional groups that can facilitate transporting fullerene through lipid

bilayer. To achieve this goal, CG-MD using the MARTINI force field has been employed. The optimization was carried out based on comparing PMF profiles.

2 Method

2.1 Coarse-grained Mapping

Our system was composed of the DPPC lipid bilayer and one fullerene immersed in water. CG mapping for the system was built according to MARTINI force field as developed by Marrink et al. [18] and composed of 4 to 1 mapping for DPPC and water molecules. As suggested by the force field, anti-freeze particles (BP4) were employed to prevent freezing with molar fraction equal to 0.1 [18].

To model fullerene, a 16-bead system of SC4 type was used as suggested by Wong-Ekkabut et al. [17] (see Fig. 1). To model the hydroxyl groups, an $-\text{OH}$ group was merged on one bead of fullerene and assigned as SP1. All the connections between beads were defined as constraints instead of harmonic bonds. In this work, we first performed a simulation to find the equilibrated location of fullerene in the system containing the DPPC bilayer. Subsequently, the PMF profile for systems containing C_{60} with/without functional groups was calculated in separate simulations (Table 1).

2.2 Molecular Dynamics Simulation

CG-MD simulations were performed using the GROMACS v. 4.5.4 MD package [19]. The system contained 89 DPPC, 8808 water, and one fullerene molecule or one of its hydroxyl derivatives. Periodic boundary conditions were used in all three Cartesian directions. Initially, the system was equilibrated for 4.0 ns in NPT condition, followed by 4.0 ns in NVT. A 20-fs time step was used to integrate the equations of motion. Nonbonded interactions was cut off at a distance of 1.2 nm. The long-range Coulomb interactions were calculated via the particle-mesh Ewald sum method with a grid spacing of approximately 1.0 Å. The temperature and pressure were controlled using the Nose-Hoover [20] and Berendsen et al. [21] algorithms, respectively. MD simulations were run at

Fig. 1 Coarse-grained model of fullerene **a** showing constraints between interaction sites **b** having 16 interaction sites to build the model according to MARTINI force field

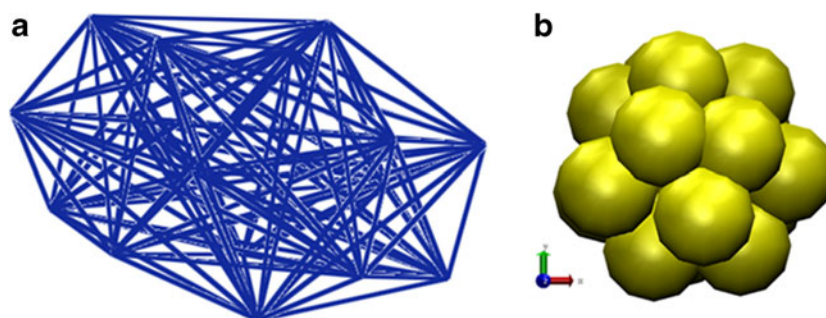


Table 1 All the systems were examined in this study

Purpose of simulation	Title	Conditions
Calculating PMF ^a	C ₆₀	C ₆₀ without any functional group
	C ₆₀ (OH) ₄	C ₆₀ with four hydroxyl groups
	C ₆₀ (OH) ₅	C ₆₀ with five hydroxyl groups
	C ₆₀ (OH) ₆	C ₆₀ with six hydroxyl groups
	C ₆₀ (OH) ₈	C ₆₀ with eight hydroxyl groups
	C ₆₀ (OH) ₁₂	C ₆₀ with 12 hydroxyl groups
	C ₆₀ (OH) ₁₆	C ₆₀ with 16 hydroxyl groups
Finding equilibrated condition	C ₆₀	200 ns run to find equilibrated location of fullerene

^a In these simulations C60 with/without functional groups has been pulled toward the center of mass (COM) of DPPC bilayer. Then, using the umbrella sampling, the PMF has been calculated for every single system

300 K in NVT ensemble. All visualizations and analyses were performed using the VMD v. 1.9 visualization tools [22].

2.3 Free Energy Calculation

The PMF was calculated for each system (i.e., fullerene and its derivatives) to estimate the free energy profiles along the reaction coordinate. A fullerene molecule was initially placed in the water region approximately 1 nm away from the bilayer in a fully hydrated DPPC bilayer system (i.e., ≈ 4 nm from the center of mass of the DPPC). The GROMACS pull code was used to pull fullerene and its derivatives in the *z*-direction (one dimensional pulling) to the bilayer center plane at a rate of 1.0 \AA ns^{-1} . All simulations were carried out at constant temperature (300 K) using semi-isotropic pressure coupling, allowing for changes in the box size in all dimensions. Thereafter, fullerene was gradually pulled, and an umbrella harmonic potential was employed as a pulling force with a force constant of $1,500 \text{ kcal mol}^{-1} \text{ \AA}^{-2}$, along with application of the umbrella sampling technique. Depending on the solute molecule (fullerene or its derivatives), 70–140 windows were

chosen between the initial and final locations of fullerene. At each separation window, the system was equilibrated for 1 ns followed by a 40-ns data collection run. Afterwards, using weighted histogram analysis method, the PMF profile and histograms were produced [23].

3 Results and Discussion

In the atomistic simulations, various force fields for fullerene modeling have been used so far, e.g., DREIDING [24], AIREBO [25], GROMACS [26], and standard Tripos molecular mechanic [27]. Additionally, a few coarse-grained force fields have been used to model fullerene so far. Chiu et al. used CG:AA carbon mapping ratio of 2:3 from the CG benzene model. In this CG model, the C₆₀ molecule contains 40 interaction sites [6]. D’Rozario et al. [16] used 3-to-1 mapping and considered 20 beads for fullerene CG model. They restrained fullerene CG model to preserve the overall shape of the molecule in a sphere with diameter of ~ 1.1 nm. In the current study, fullerene was modeled based on the model proposed by Wong-Ekkabut et al. [17] with 16 interaction sites, taking advantage of being more comparable with atomistic results [11, 13].

In the longer run for C₆₀ (200 ns), the *z*-direction movement of fullerene towards the bilayer and its jump into the bilayer and movement between two leaflets are shown in Fig. 2. Initially, fullerene was located outside the membrane at 2 nm distance from head group of the DPPC molecules. During the first ~ 60 ns, the fullerene slowly moves towards the bilayer, then makes contact with the lipid bilayer. During the next 20 ns, C₆₀ “jumps” into the bilayer and is finally located ~ 1 nm from the bilayer center. This finding is in good agreement with atomistic MD results [11, 13], indicating suitability of the model used for fullerene in this study.

Figure 3 shows some snapshots of pulling fullerene into the membrane in four stages. In Fig. 3a, fullerene has been

Fig. 2 *z*-direction movements of C₆₀ toward the bilayer, jumping to bilayer, and following movements inside the bilayer, as functions of time; distances are measured from according to center of bilayer

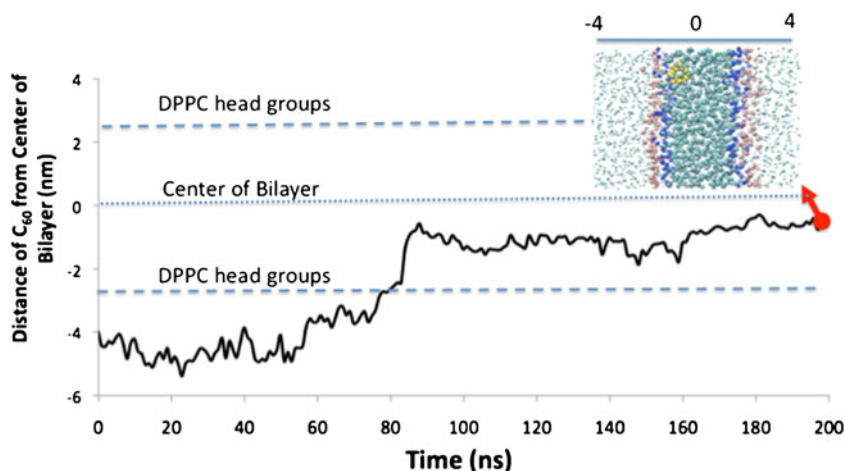
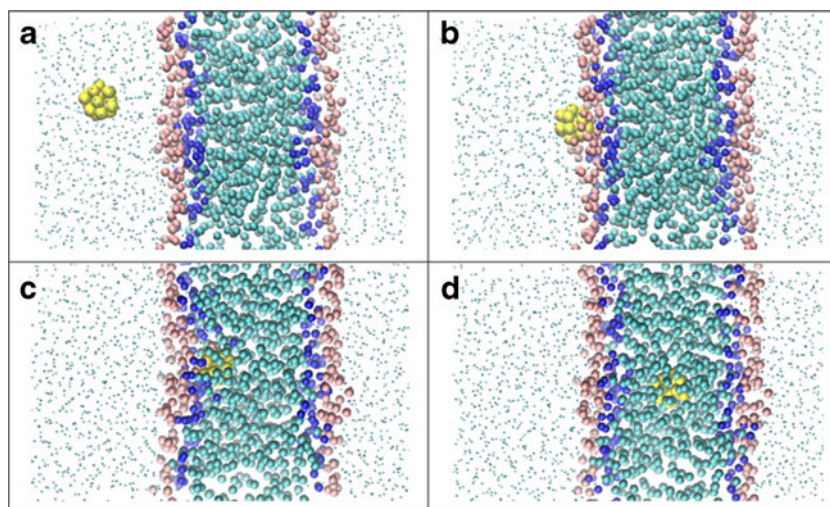


Fig. 3 Snapshots of the pull process to calculate the PMF when fullerene is located **a** outside, **b** near outer periphery, **c** near inner periphery, and **d** at the center of bilayer



illustrated outside the membrane. Figure 3b shows the particle when it is located at the outer periphery of the membrane interacting with hydrophilic head groups of DPPC molecules. Clearly, C_{60} creates disorders in head groups when moving towards the center of bilayer. In Fig. 3c, the fullerene is interacting with intermediate hydrophilic groups in bilayer and tail groups. Finally, C_{60} is locating inside the membrane as shown in Fig. 3d.

Figure 4 shows the PMF profiles of fullerene and its hydroxyl derivatives with 4, 8, 12, and 16 –OH groups. According to the atomistic simulations performed by Qiao et al. [12] when crossing the lipid bilayer, the minimum value for the PMF is located approximately 1.2 nm from the center of bilayer. Moreover, Li et al. [11] using AA-MD illustrated that fullerene is located 6–7 Å off-center in DMPC which is in agreement with the results of Bedrov et al. [13] using a similar

technique. The C_{60} PMF profile in Fig. 4 clearly identifies similar stable position for fullerene. However, previous CG-MD results [16] showed that the location of the fullerene at equilibrium state is at the center of the membrane, contradicting the off-center stable location suggested by atomistic simulations.

The lowest PMF value reported using interatomic force field is ~22 kcal at 310 K for DMPC [13] and ~10 kcal at 325 K for DPPC [12]. Here, this value is approximately 20 kcal at 300 K. The difference in the obtained values may be due to the approximations employed in CG-MD to increase computational efficiency. Reviewing the literature, there is a single CG result for DPPC at 323 K which shows ~–48 kcal for the lowest PMF [16]. Thus, the results of our CG model are reliable from the viewpoint of mimicking the behavior of C_{60} and its derivatives when passing through the lipid bilayer.

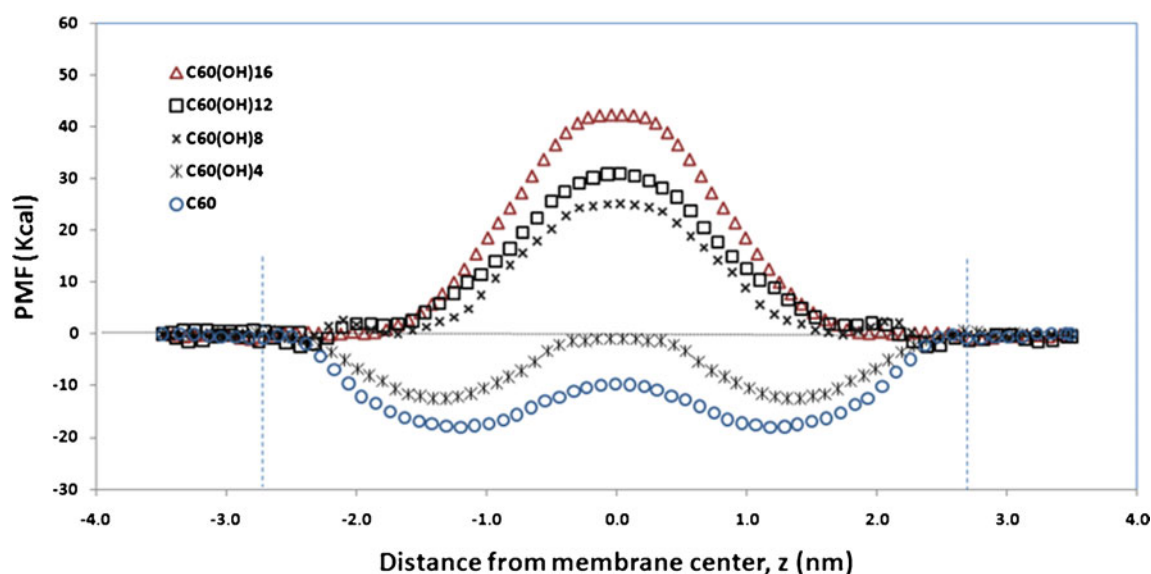


Fig. 4 PMF profiles of fullerene and its hydroxyl derivatives with 4, 8, 12, and 16 –OH groups. Zero on horizontal axis shows the membrane center in the z -direction and vertical dashed lines represent approximate location of the membrane leaflets (head groups of DPPC molecules)

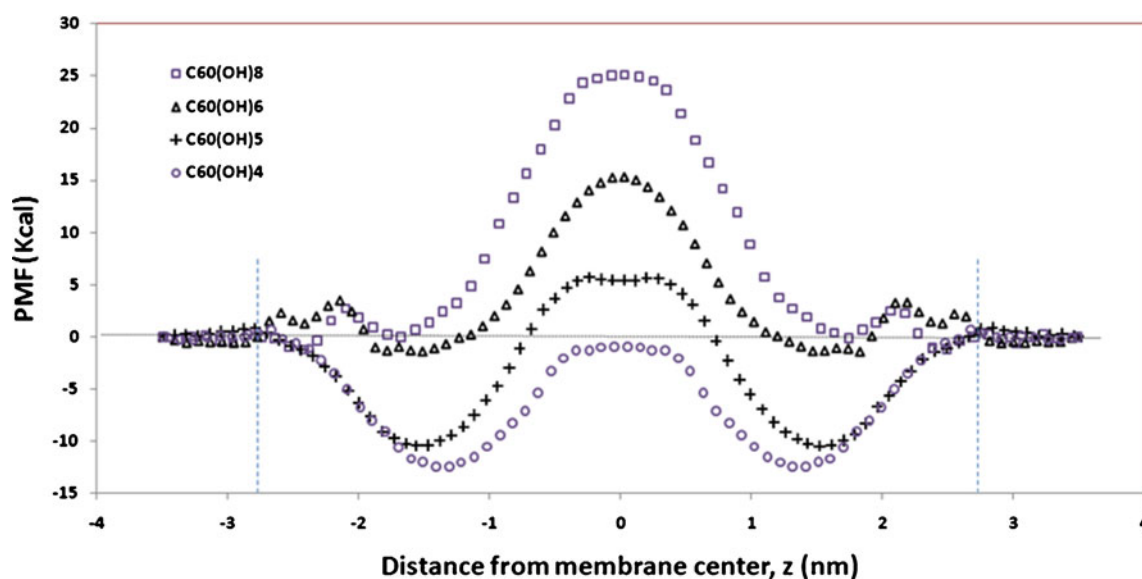


Fig. 5 Comparison of the PMF profiles of fullerene hydroxyl derivatives with 4, 5, 6, and 8 -OH groups

Among the plots in Fig. 4, the optimal choice in crossing the DPPC bilayer should be the one that has the smallest difference between the peak and the trough of the PMF profile. Details in Fig. 4 show that C_{60} has a deep valley, while the plots for $C_{60}(\text{OH})_{12}$ and $C_{60}(\text{OH})_{16}$ indicate high peaks; thus, none could be considered as appropriate for crossing the bilayer. Hence, the best option is probably $C_{60}(\text{OH})_4$, $C_{60}(\text{OH})_8$, or a similar derivative with 4 to 8 -OH groups. Figure 5 shows the PMF profile of four to eight hydroxylated C_{60} molecules. The differences between peak and valley for $C_{60}(\text{OH})_4$, $C_{60}(\text{OH})_5$, $C_{60}(\text{OH})_6$, and $C_{60}(\text{OH})_8$ are about 12, 17, 17, and 25 kcal, respectively. Detailed comparison shows that $C_{60}(\text{OH})_4$ is as the optimal derivative,

showing the smallest difference between peak and valley (i.e., 12 kcal).

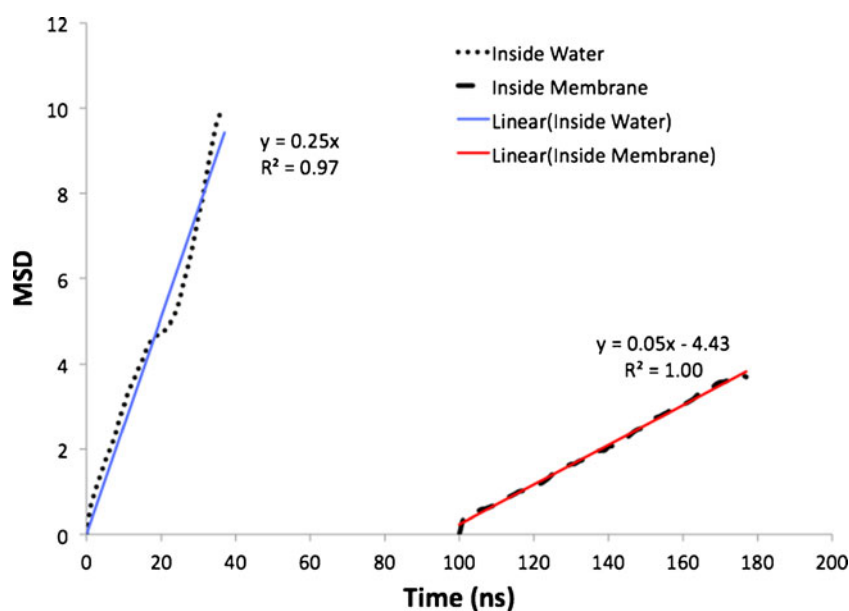
In order to study the diffusion constant of the fullerene in water and inside the membrane, the fullerene mean square displacement (MSD) in each phase has been calculated separately (see Fig. 6).

According to the Einstein relation [28]:

$$\lim_{t \rightarrow \infty} \left\langle \|r_i(t) - r_i(0)\|^2 \right\rangle_{i \in A} = 6D_A t,$$

where $r_i(t) - r_i(0)$ is the distance traveled by molecule i over a time interval of length t and D_A is the diffusion

Fig. 6 Mean square displacement (MSD) of the center of the mass of fullerene inside water and bilayer



coefficient of species A. The number 6 indicates dimensionality; 2, 4, or 6 for 1, 2, or 3 dimensional diffusion, respectively. As in this report the three-dimensional MSD has been calculated, the dimensionality number in the equation should be 6. Comparison between the slopes of the two plots clearly demonstrates that the self-diffusivity of fullerene inside water is higher than in the membrane. It should be mentioned that the water diffusivity of fullerene in this case may be different from its diffusivity in bulk water. The different diffusivities of the fullerene in these two media may be associated with the differences in the physicochemical interactions of the molecules. Especially, hydrophobic interactions between the hydrophobic fullerene and the acyl chains of DPPC molecules prevent free movements of C_{60} inside the membrane. We conclude that the bilayer provides a more viscous medium for fullerene movements.

Similar studies for the z -direction movement of $C_{60}(OH)_4$ were performed comparing the results with those for C_{60} . However, during a 200-ns simulation, the molecule did not appear to move towards the bilayer. It is arguable that since the C_{60} is not water soluble, the water medium “pushes” the C_{60} to the bilayer; thus, this particle is able to overcome the energy barrier observed at the periphery of the bilayer. By contrast, the water solubility of the optimal hydroxyl derivative (i.e., $C_{60}(OH)_4$) is substantially higher. Therefore, the particle is not able to pass the energy barrier and move towards the center of the bilayer.

4 Conclusion

Using the force field suggested by Wong-Ekkabut et al. to investigate the behavior of fullerene and its derivatives, we have obtained results in closer agreement with atomistic simulations than previous CG-MD studies. Although the center of the bilayer is the lowest density region, the hydrophobic fullerene prefers to be located off-center of the DPPC membrane. This position for C_{60} is in agreement with the findings from the AA-MD approach. Among hydroxyl derivatives of fullerene, $C_{60}(OH)_4$ showed the lowest difference between peak and valley (i.e., the most suitable free energy profiles to pass through the bilayer). This derivative can facilitate transporting C_{60} through the bilayer membrane. As the average self-diffusivity of fullerene inside the bilayer is substantially smaller than in the water, the bilayer appears to provide a more viscous medium for fullerene.

References

1. Z. Zhu, D.I. Schuster, M.E. Tuckerman, Molecular dynamics study of the connection between flap closing and binding of fullerene-based inhibitors of the HIV-1 protease. *Biochem.* **42**, 1326–1333 (2003)
2. S. Bosi, T.D. Ros, G. Spalluto, J. Balzarini, M. Prato, Synthesis and anti-HIV properties of new water-soluble bis-functionalized[60]fullerene derivatives. *Bioorg. Med. Chem. Lett.* **13**, 4437–4440 (2003)
3. R. Bakry, R.M. Vallant, M. Najam-ul-Haq, M. Rainer, Z. Szabo, C.W. Huck, G.K. Bonn, R. Bakry, R.M. Vallant, M. Najam-ul-Haq, M. Rainer, Z. Szabo, C.W. Huck, G.K. Bonn, Medicinal applications of fullerenes. *Int J Nanomed* **2**, 639–649 (2007)
4. A.W. Jensen, S.R. Wilson, D.I. Schuster, Review article: biological applications of fullerenes. *Bioorg. Med. Chem.* **4**, 767–779 (1996)
5. S. Bosi, T.D. Ros, G. Spalluto, M. Prato, Fullerene derivatives: an attractive tool for biological applications. *Eur. J. Med. Chem.* **38**, 913 (2003)
6. C. Chiu, R. DeVane, M.L. Klein, W. Shinoda, P.B. Moore, S.N. Nielsen, Coarse-grained potential models for phenyl-based molecules: II. Application to fullerenes. *J. Phys. Chem. B* **114**, 6394–6400 (2010)
7. R. DeVane, A. Jusufi, W. Shinoda, C. Chiu, S.O. Nielsen, P.B. Moore, M.L. Klein, Parametrization and application of a coarse grained force field for benzene/fullerene interactions with lipids. *J. Phys. Chem. B* **114**, 16364–16372 (2010)
8. D.Y. Lyon, L.K. Adams, J.C. Falkner, P.J.J. Alvarez, Antibacterial activity of fullerene water suspensions: effects of preparation method and particle size. *Environ. Sci. Technol.* **40**, 4360–4366 (2006)
9. C.M. Sayes, J.D. Fortner, W. Guo, D. Lyon, A.M. Boyd, K.D. Ausman, Y.J. Tao, B. Sitharaman, L.J. Wilson, J.B. Hughes, J.L. West, V.L. Colvin, The differential cytotoxicity of water-soluble fullerenes. *Nano Lett.* **4**, 1881–1887 (2004)
10. Y. Chang, C. Chunying, Y. Chang, C.C. Chunying, M. Zhen, X. Huan, J. Li, Y. Yaxin, X. Hui, Z. Gengmei, Z. Feng, C. Yuliang, F. Zhifang, H. Xiaohong, C. Dong, W. Long, W. Chen, W. Taotao, In situ observation of $C_{60}(C(COOH)_2)_2$ interacting with living cells using fluorescence microscopy. *Chin. Sci. Bull.* **51**, 1060–1064 (2006)
11. L. Li, H. Davande, D. Bedrov, G.D. Smith, A molecular dynamics simulation study of C_{60} fullerenes inside a dimyristoylphosphatidylcholine lipid bilayer. *J. Phys. Chem. B* **111**, 4067–4072 (2007)
12. R. Qiao, A.P. Roberts, A.S. Mount, S.J. Klaine, P.C. Ke, Translocation of C_{60} and its derivatives across a lipid bilayer. *Nano Lett* **7**, 614–619 (2007)
13. D. Bedrov, G.D. Smith, H. Davande, L. Li, Passive transport of C_{60} fullerenes through a lipid membrane: a molecular dynamics simulation study. *J. Phys. Chem. B* **112**, 2078–2084 (2008)
14. M.S.P. Sansom, K.A. Scott, P.J. Bond, Coarse-grained simulation: a high-throughput computational approach to membrane proteins. *Biochem. Soc. Trans.* **36**(1), 27–32 (2008)
15. S.O. Nielsen, C.F. Lopez, G. Srinivas, M.L. Klein, Coarse grain models and the computer simulation of soft materials. *J. Phys.: Condens. Matter* **16**, R481–R512 (2004)
16. R.S.G. D’Rozario, C.L. Wee, E.J. Wallace, M.S.P. Sansom, The interaction of C_{60} and its derivatives with a lipid bilayer via molecular dynamics simulations. *Nanotechnol.* **20**, 102–115 (2009)
17. J. Wong-Ekkabut, S. Baoukina, W. Triampo, I.M. Tang, D.P. Tieleman, L. Monticelli, Computer simulation study of fullerene translocation through lipid membranes. *Nat. Nanotechnol.* **3**, 363–368 (2008)
18. S.J. Marrink, H.J. Risselada, S. Yefimov, D.P. Tieleman, A.H. Vries, The MARTINI force field: coarse grained model for biomolecular simulations. *J. Phys. Chem. B* **111**, 7812–7824 (2007)
19. S. Pronk, S. Páll, R. Schulz, P. Larsson, P. Bjelkmar, R. Apostolov, M.R. Shirts, J.C. Smith, P.M. Kasson, D. van der Spoel, B. Hess, Erik Lindahl, GROMACS 4.5: a high-throughput and highly parallel open source molecular simulation toolkit. *Bioinforma.* **29**(7), 845–854 (2013)
20. D.J. Evans, B.L. Holian, The Nose–Hoover thermostat. *J. Chem. Phys.* **85**, 4069–4074 (1985)
21. H.J.C. Berendsen, J.P.M. Postma, W.F. van Gunsteren, A. DiNola, J.R. Haak, Molecular dynamics with coupling to an external bath. *J. Chem. Phys.* **81**, 3684–3690 (1984)

22. W. Humphrey, A. Dalke, K. Schulten, VMD—visual molecular dynamics. *J. Mol. Graphics* **14**, 33–38 (1996)
23. S. Kumar, J.M. Rosenberg, D. Bouzida, R.H. Swendsen, P.A. Kollman, The weighted histogram analysis method for free-energy calculations on biomolecules. I. The method. *J. Comput. Chem.* **13**, 1011–1021 (1992)
24. P.S. Redmill, S.L. Capps, P.T. Cummings, C. McCabe, A molecular dynamics study of the Gibbs free energy of solvation of fullerene particles in octanol and water. *Carbon* **47**, 2865–2874 (2009)
25. B. Czerwinski, L. Rzeznik, K. Stachura, R. Paruch, B.J. Garrison, Z. Postawa, Applications of fullerene beams in analysis of thin layers. *Vacuum* **82**, 1120–1123 (2008)
26. K. Tappura, O. Cramariuc, T.L.J. Toivonen, T.I. Hukka, T.T. Rantala, Computational analysis of the conformations of a doubly linked porphyrin–fullerene dyad. *Chem. Phys. Lett.* **424**, 156–161 (2006)
27. S. Durdagi, T. Mavromoustakos, N. Chronakis, M.G. Papadopoulos, Computational design of novel fullerene analogues as potential HIV-1 PR inhibitors: analysis of the binding interactions between fullerene inhibitors and HIV-1 PR residues using 3D QSAR, molecular docking and molecular dynamics simulations. *Bioorg. Med. Chem.* **16**, 9957–9974 (2008)
28. M.P. Allen, D.J. Tildesley, *Computer simulation of liquids* (Oxford University, USA, 2002)